

Fermi surface of α -uranium at ambient pressure

D. Graf,¹ R. Stillwell,¹ T. P. Murphy,¹ J.-H. Park,¹ M. Kano,¹ E. C. Palm,¹ P. Schlottmann,² J. Bourg,² K. N. Collar,² J. C. Cooley,³ J. C. Lashley,³ J. Willit,⁴ and S. W. Tozer¹

¹National High Magnetic Field Laboratory, Florida State University, Tallahassee, Florida 32310, USA

²Department of Physics, Florida State University, Tallahassee, Florida 32306, USA

³Materials Science and Technology Division, Los Alamos National Laboratory, Los Alamos, New Mexico 87545, USA

⁴Argonne National Laboratory, Argonne, Illinois 60439, USA

(Received 27 October 2009; published 4 December 2009)

We have performed de Haas–van Alphen measurements of the Fermi surface of α -uranium single crystals at ambient pressure within the α_3 charge-density wave (CDW) state from 0.020–10 K and magnetic fields to 35 T using torque magnetometry. The angular dependence of the resulting frequencies and the effective masses were measured. The observation of quantum oscillations within the α_3 CDW state gives insight into the effect of the charge-density waves on the Fermi surface. We observed no signature of superconductivity in either transport or magnetization down to 0.020 K at ambient pressure.

DOI: [10.1103/PhysRevB.80.241101](https://doi.org/10.1103/PhysRevB.80.241101)

PACS number(s): 71.18.+y, 71.45.Lr

Uranium has remained a challenge for condensed-matter physics since the first scientific work on it more than a century ago. The orthorhombic alpha phase of uranium (α -U) provides a unique setting to understand the role of f -electrons in the complex behavior of the actinides. The three low-temperature charge-density wave transitions, located at 43 (α_1), 37 (α_2), and 23 K (α_3), result in the volume of the unit cell below 23 K growing by a factor of 72 to $\sim 6000 \text{ \AA}^3$.¹ Uranium also undergoes high-temperature phase transitions to the beta and gamma structures that render it impossible to grow high-quality single crystals of the alpha phase by the usual methods. In addition, the crystal structure of α -U resembles corrugated cardboard along the [001] direction² making the crystal particularly susceptible to twinning or sliding along the [100] axis due to the (010) glide plane.¹ Single crystals were serendipitously grown at Argonne National Laboratory while separating uranium from fission products in an experiment regarding uranium fuel refinement.³ These crystals proved to be of much higher quality than any previously available and provided insights into the physics of α -U.^{4,5} Although many outstanding questions remain including the origin of the charge-density wave (CDW) transitions, superconductivity and the unique crystal structure, one issue is viewed as being a key to understanding the rest: the determination of the electronic structure of α -uranium. Here we report ambient pressure de Haas–van Alphen (dHvA) measurements of high-quality crystals of α -U that have been enhanced with an annealing procedure to produce residual resistivity ratios (RRR) of up to 570, doubling the previous record.⁴ Improved magnetic torque measurement techniques and DC fields to 35 T allowed the observation of at least ten distinct frequencies for α -U with effective masses less than or equal to 1.62 m_e . The quantum oscillations are observed after passing through the three CDW transitions shedding light on the nature of the CDW's and their effect on the Fermi surface of α -U.

Charge-density waves are quite common in a number of other materials, e.g., NbSe₃,⁶ Cr,⁷ blue bronze,⁸ organic conductors,⁹ and TaSe₂.¹⁰ These collective modes are usually associated with reduced dimensionality whereas U is a three-dimensional metal with a low-symmetry structure. In Cr the charge-density wave appears in conjunction with a spin-

density wave over a small temperature interval.⁷ The CDW's in α -U are a result of Peierls distortions, due to Fermi-surface nesting of the complex band structure of the f -states.¹¹ The CDW's in α -U have historically made the observation of quantum oscillations quite difficult due to the concomitant stress and defects that were predicted to damage the crystal.¹⁴ To observe dHvA oscillations was thought to be impossible without suppressing the CDW state via pressure because they require very clean crystals with long electron mean-free paths. This was the motivation for the seminal high-pressure dHvA measurements of Schirber and Arko.¹²

Our measurements were carried out in a variety of systems including an Oxford top loading dilution refrigerator located in a 35 T resistive magnet, a Janis variable-temperature insert (VTI) housed in a 31 T resistive magnet, a Quantum Design PPMS with a 16 T superconducting magnet and a Oxford top loading dilution refrigerator with a 20 T superconducting magnet. The α -U crystals were from a 1997 electrometallurgical growth using electrotransport through a LiCl-KCl eutectic flux containing 3% UCl₃ by weight.³ The resistance as a function of temperature of an annealed sample is shown in Fig. 1 and the three CDW transitions are manifested in this data as steps at 43, 37, and 23 K as has been previously observed.^{4,5} They are more clearly seen in the dR/dT plot shown in the top panel of the figure. As seen in the inset to Fig. 1, the RRR is clearly enhanced from a typical unannealed value of 1–5 to a value of 570 indicating the low scattering rate in these crystals. Repeated thermal cycling from 300 to 4 K did not degrade the RRR and the traces clearly showed hysteresis in the 23 K transition as observed in prior work.⁴ The plateau at 180 K has been observed in several crystals, but a cause has not yet been determined. The crystals were oriented using both Laue x-ray backscatter and single-crystal x-ray diffraction. Seiko piezo cantilevers were used to observe the quantum oscillations in all the magnet systems described above. A metal foil cantilever was also used to observe these oscillations using a dilution refrigerator in a 35 T resistive magnet and 20 T superconducting magnet. While the data were not of a comparable quality and are not reported here, these measurements did

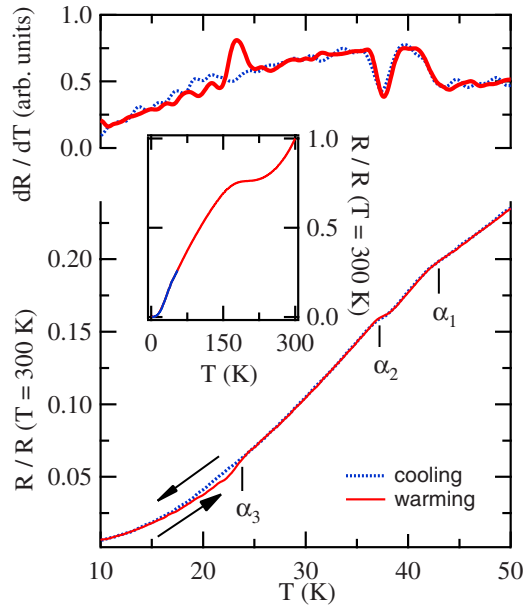


FIG. 1. (Color online) The zero-field resistivity and its derivative showing charge-density wave transitions α_1 , α_2 , and α_3 at 43, 37, and 23 K, respectively. Inset shows the overall resistivity change from room temperature to 1.8 K with RRR=570.

play the important role of confirming the results obtained using the piezo cantilevers.

Multiple crystals from multiple anneals were used for this study. All experiments below 1.4 K were performed with samples located in the dilute solution of the dilution refrigerators. From previous experience with self heating due to the radioactive decay of a ^{60}Co single crystal of similar size and with a much higher total activity, the resulting self heating in $\alpha\text{-U}$ could only lead to a maximum temperature rise to 60 mK at the sample with the surrounding dilute mixture at 20 mK. Since the highest observed effective mass was $1.62 m_e$ and the Dingle temperature was found to be of the order of 1 K, we conclude that radioactive self heating was not significant for our experiments.

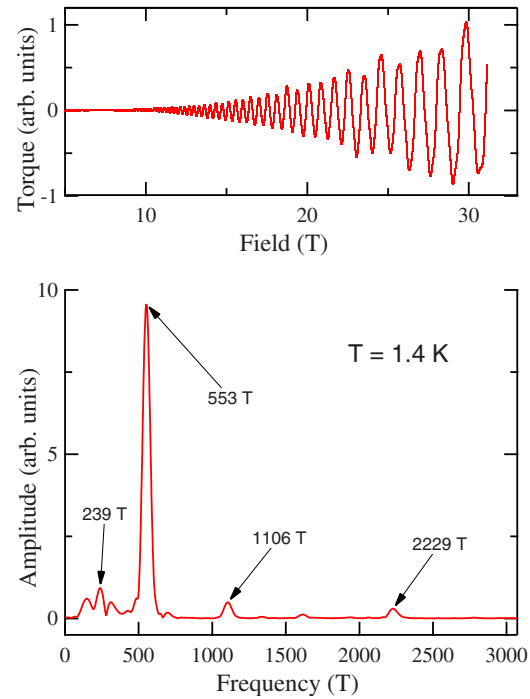


FIG. 2. (Color online) FFT result on background subtracted torque signal (top panel). The angle of the applied field is 65° off [100] rotating toward [001].

Figure 2 shows a representative torque signal from a magnetic field sweep with the background subtracted for a misalignment of 65° from the [100] axis toward the [001] axis at 1.4 K. This angle was chosen because the observed torque signal becomes smaller as the field is aligned along one of the principal axes due to the alignment of the magnetization vector with the applied field. Oscillations are clearly visible (top panel) and a fast Fourier transform (FFT) analysis reveals multiple frequencies. The large amplitude of the quantum oscillations shows the low scattering rate of the crystals used in this study.

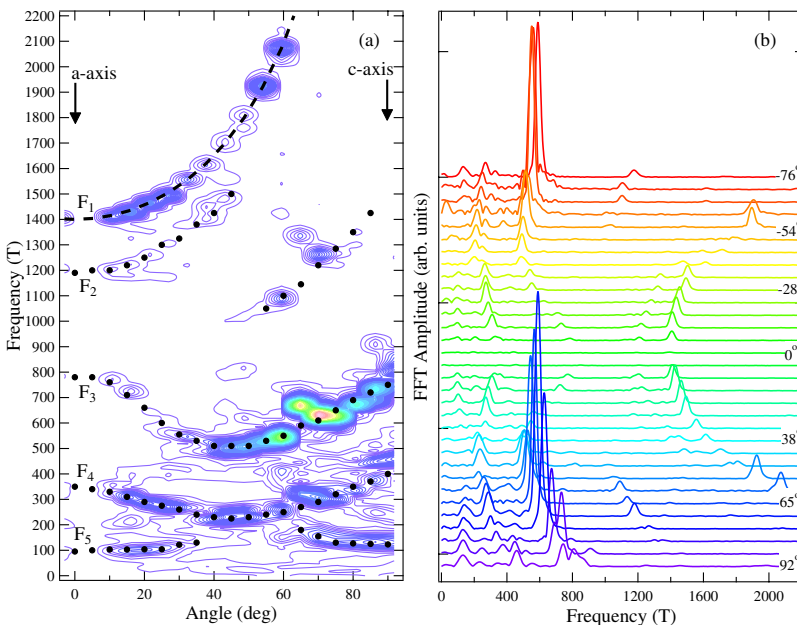


FIG. 3. (Color online) FFT results from background subtracted torque signal taken with the field aligned (a) between [100] and [001] axes for $T \sim 1.4$ K. The contour plot shows black dots at selected frequency peaks as a guide for the eye. Colors on the contour plot represent amplitude of the FFT at fixed angle with red being the largest values. The black dashed line in 3a represents a $1400/[\cos(X\theta)]$ fit to the F_1 (β) orbit, (where $X \sim 0.8$) in agreement with the work of Schirber and Arko (Ref. 12). (b) A waterfall plot of the FFTs taken for a series of angles $\sim 6^\circ$ apart.

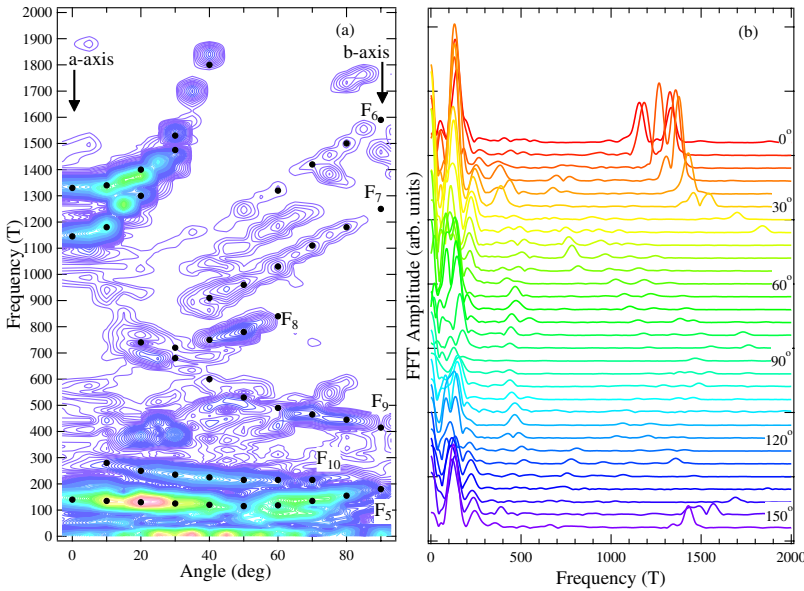


FIG. 4. (Color online) FFT results from background subtracted torque signal at angles between $[100]$ and $[010]$, with the rotational axis parallel to $[001]$ and a temperature of 1.8 K. (a) A contour plot with solid black dots at selected frequency peaks and the color red representing the largest FFT amplitude. (b) A waterfall plot of the FFT for a series of angles. The offset is proportional to an angular difference of 5° between traces.

In order to investigate the Fermi surface of α -U the orientation of the crystal was set via a rotation platform between $[100]$ and $[001]$ and also $[100]$ to $[010]$, and then the magnetic field was swept. Figures 3 and 4 show the angular dependence of the frequencies at various orientations. The intensity of the frequency peaks is indicated in the contour plots as color changes and dotted lines are shown as a guide to the eye. The observed Fermi surface has more frequencies than those seen at high pressure by Schirber and Arko, especially frequencies below 500 T. The origin of these frequencies could be small unnested portions of the Fermi surface at ambient pressure or the large magnetic fields available (i.e., 31 T) for our measurements, allowing us to push 21 T past the work of Schirber and Arko.

The surface described by the F_1 peak, when the field is aligned near the a-axis, is very similar to the β orbit found by Schirber and Arko.¹² The angular dependence of the frequency changes more slowly than a cylinder (i.e., $F_0/\cos \theta$ where F_0 is the minimum and θ is the angle between the field and the minimum) when rotated from $[100]$ toward $[001]$, which also agrees with their findings. Interestingly, this orbit frequency changes more quickly than a cylinder when rotated toward $[010]$. It appears at least this portion of the Fermi surface is less sensitive to the presence of the CDWs or applied pressure. The latter is supported by an anisotropic linear compressibility which is weakest along the a-axis when hydrostatic pressure is applied, due to the anisotropic interatomic spacing.¹³ This may lead to more pronounced differences between measured orbits for ambient and applied pressure when the magnetic field is orthogonal to the a-axis. Along this line, F_3 becomes the dominant frequency of the FFT spectrum as the sample is rotated away from $[100]$ toward $[001]$ suggesting this orientation is more susceptible to changes from the CDW formation or applied pressure.

The differences in observed Fermi surfaces between this work and those of reference 12 show the role played by restructuring due to the charge-density waves, lattice changes from applied pressure, and the higher sensitivity of the measurement techniques used in this study. Given that the vol-

ume of the unit cell grows to 6000 \AA^3 in the α_3 state,¹ it is not surprising that there are differences in the frequencies observed at ambient and high pressures.

The effective masses for some of the measured frequencies were determined by the Lifshitz-Kosevich relation from the temperature dependences of the frequency peaks.¹⁴ These masses and frequencies are shown in Tables I–III. The measured effective masses ($\sim 1.6 m_e$) are consistent with the Schirber and Arko work, as well as with measurements of the specific heat that determine $\gamma=9.13 \text{ mJ}/(\text{mol K}^2)$.⁵ This value and generalized gradient approximation (GGA) calculations¹⁵ of the band structure provide a mass enhancement limit of ~ 1.55 . The frequencies reported here have proven to be reproducible in a number of samples. A Dingle temperature of $\sim 1.6 \text{ K}$ was determined from one such sample, which was produced using the same annealing process as the RRR ~ 570 sample.

Several theoretical papers have attempted to calculate the physical properties of α -U,^{11,16,17} but a direct comparison with low-temperature estimates of the Fermi surface is not yet available (one that takes into account all three CDW transitions). Only the transition from the alpha to the α_1 phase appears to be understood due to nesting between parallel Fermi-surface sections.¹¹ There also exist conjectures on the second transition, i.e., from the α_1 phase to the α_2 phase.¹¹ With the most pronounced lattice distortion (α_1) taken into account, there seems to be some agreement be-

TABLE I. Measured dHvA frequencies and effective masses with H applied $\sim 12^\circ$ off $[100]$ rotating toward $[001]$.

Symbol	Frequency (T)	m^*/m_0
F_1	1402	1.23
F_2	1190	1.06
F_3	780	1.33
F_4	360	0.94
F_5	98	0.68

TABLE II. Measured dHvA frequencies and effective masses with H applied along $[001]$.

Symbol	Frequency (T)	m^*/m_0
F ₃	750	1.62
F ₄	400	1.37
F ₅	120	0.59

tween the ~ 860 T central feature of the Fermi surface shown in Fig. 3b of Ref. 11 and the ~ 700 T frequency we find with the field aligned with the c -axis. Without further information about the overall shape of the Fermi surface, it is impossible to say if this is a coincidence. In an attempt to explain the results of Ref. 12, Yamagami and Hasegawa¹⁶ calculated the Fermi surface for α -U and shifted the Fermi level of their results to find the best agreement with Schirber and Arko's work. The calculated frequencies were higher than those found in Ref. 12 and much higher than those found in the present study. This discrepancy is likely from the effect of the CDW transition on the Fermi surface, which not included in the calculations. There is still much to understand regarding the f -electron behavior and having experimental evidence of the electronic structure could aid in modeling efforts.

Preliminary resistance and magnetization measurements to 20 mK on our samples showed no signs of the filamentary or bulk superconductivity previously reported at ambient pressure between 0.1 to 1.3 K.^{1,4,18} It has been posited that the superconductivity in α -U is a result of strain on grain boundaries where T_c is suppressed in cleaner samples^{1,4} so it is possible that the internal strain in our annealed samples was low enough to prevent superconductivity.¹ Given the large RRR and the lack of a superconducting transition in the present work the hypothesis that superconductivity at ambient pressure in α -U is impurity driven seems plausible. The present scenario would then be that the application of pressure suppresses the CDWs and that α -U has a pressure-induced superconducting dome. Therefore, it is possible that at low temperatures a pressure-tuned quantum critical point separates the normal phase from the superconducting phase.

In conclusion we observed a rich set of orbits for α -U in the ambient pressure α_3 charge-density wave phase. These

TABLE III. Measured dHvA frequencies with H along $[010]$. F₈ is only visible starting from 30° off of $[010]$ rotating toward $[100]$.

Symbol	Frequency (T)
F ₅	175
F ₆	1410
F ₇	1350
F ₈	920
F ₉	430
F ₁₀	215

results show that the distortions of the lattice due to CDWs do not prevent the observation of quantum oscillations. This may be because in general materials that display CDWs are themselves very sensitive to strain which in the present case may have been reduced by the process of annealing the α -U crystals. This process, coupled with the increased sensitivity of the cantilever measurements, enabled the observation of dHvA oscillations in α -U at ambient pressure. Unfortunately, no calculation of the Fermi surface of the α_3 phase is available at this point so that a comparison between the measured and the theoretical Fermi surface is not possible. The small effective masses found by Schirber and Arko under pressure have been confirmed, suggesting that α -U is not a strongly correlated system. Superconductivity was not observed via resistivity or torque magnetometry down to 0.020 K in the high-quality crystals used in this study supporting the view that superconductivity in α -U at ambient pressure is induced by defects and/or impurities. Further experiments are underway to follow the evolution of the Fermi surface with pressure to connect with the work by Schirber and Arko.

The authors would like to thank Jim Schirber and Jim Smith for useful discussions and historical notes and Vaughn Williams and Robert Schwartz for technical support. Support for this work was provided by the DOE/NNSA under Grant No. DE-FG52-06NA26193. This work was performed at the National High Magnetic Field Laboratory which is supported by NSF Cooperative Agreement No. DMR-0654118 and by the State of Florida. P.S. is supported by the DOE under Grant No. DE-FG02-98ER45707.

¹G. H. Lander, E. S. Fisher, and S. D. Bader, *Adv. Phys.* **43**, 1 (1994).

²L. T. Lloyd and C. S. Barrett, *J. Nucl. Mater.* **18**, 55 (1966).

³C. C. McPheeters, E. C. Gay, E. J. Karell, and J. P. Ackerman, *JOM* **49**, 22 (1997).

⁴G. M. Schmiedeshoff *et al.*, *Philos. Mag.* **84**, 2001 (2004).

⁵J. C. Lashley *et al.*, *Phys. Rev. B* **63**, 224510 (2001).

⁶M. Ido, Y. Okayama, T. Ijiri, and Y. Okajima, *J. Phys. Soc. Jpn.* **59**, 1341 (1990).

⁷E. Fawcett, *Rev. Mod. Phys.* **60**, 209 (1988).

⁸J. P. Pouget, C. Noguera, A. H. Moudden, and R. Moret, *J. Phys.* **46**, 1731 (1985).

⁹D. Jérôme and H. J. Schulz, *Adv. Phys.* **51**, 293 (2002).

¹⁰D. E. Moncton, J. D. Axe, and F. J. Disalvo, *Phys. Rev. B* **16**,

801 (1977).

¹¹L. Fast, O. Eriksson, B. Johansson, J. M. Wills, G. Straub, H. Roeder, and L. Nordstrom, *Phys. Rev. Lett.* **81**, 2978 (1998).

¹²J. E. Schirber and A. J. Arko, *Phys. Rev. B* **21**, 2175 (1980).

¹³E. S. Fisher and H. J. McSkimin, *Phys. Rev.* **124**, 67 (1961).

¹⁴D. Shoenberg, *Magnetic Oscillations in Metals* (Cambridge University Press, New York, 1984).

¹⁵C. P. Opeil *et al.*, *Phys. Rev. B* **75**, 045120 (2007).

¹⁶H. Yamagami and A. Hasegawa, *J. Phys. Soc. Jpn.* **59**, 2426 (1990).

¹⁷A. N. Chantis, R. C. Albers, M. D. Jones, M. van Schilfgaarde, and T. Kotani, *Phys. Rev. B* **78**, 081101 (2008).

¹⁸J. L. O'Brien *et al.*, *Phys. Rev. B* **66**, 064523 (2002).